Inst. Phys. Conf. Ser. No 100: Section 3
Paper presented at Microsc. Semicond. Mater. Conf., Oxford, 10–13 April 1989

Dislocation engineering in advanced III-V device structures

P Kightley, R I Taylor, A J Moseley, P D Augustus, A C Marshall and R J M Griffiths

Plessey Research Caswell Ltd, Allen Clarke Research Centre, Caswell, Towcester, Northants, NN12 8EQ.

ABSTRACT: Novel graded buffer layers have been used in the formation of lattice mismatched, low defect density, GaInAs PIN photodetectors for radiation in excess of 2 microns. TEM observation of misfit dislocation formation has enabled samples to be designed to reduce threading defect densities by forcing pre-existing and generated dislocations into lattice misfit relieving orientations. Devices displayed better than 95% peak quantum efficiency over the 1.7 to 2.2 micron wavelength range with leakage currents as low as 35 nA at -0.5V.

1. INTRODUCTION

Many advanced device applications have been designed for III-V materials incorporating layers that are mismatched from the substrate. Demand for infra-red detectors in the 1.0 to 1.6 micron wavelength range is easily satisfied by photodiodes fabricated from lattice matched $Ga_xIn_{1-x}As$ grown onto InP substrates. However, for future communications systems, based on novel fluoride fibres, detectors operating in excess of 2 microns wavelength are required. To enable this GaInAs PIN photodiodes have been fabricated using higher indium content alloys. The principal objective was to produce high peak quantum efficiencies in the 1.6 to 2.2 micron wavelength range. The active device consists of a $Ga_xIn_{1-x}As/Al_yIn_{1-y}As/Ga_xIn_{1-x}As$ structure where x=y=0.28. The materials growth and device fabrication have been reported elsewhere [Moseley et al (1986), Scott et al (1986)].The mismatch in lattice constants, f, between the active device and the substrate has been calculated as f=0.013. The lattice mismatch due to mismatch of thermal expansion coefficients [Bisaro et al (1979)], f'_{max}, has been calculated as $f'_{max}\leq 0.0001$ and was considered as negligible. A theoretical analysis of the stresses generated during growth and the energetics of plastic deformation can be determined. This should enable us to predict the precise stress content of a layer of given composition and thickness and to calculate the point of transition from pseudomorphism to a lattice misfitted structure [Van der Merwe (1963), Matthews (1975), Van der Leur (1988)]. This loss of coherence depends upon the introduction of dislocations which may come from a variety of sources. The actual point of transition will be different for different nucleation mechanisms and also for different densities of dislocations threading up from the substrate. If a single, lattice mismatched, epitaxial layer is grown onto a substrate the layer will be purely elastically strained if its thickness is less than the critical thickness, whereas, if the layer thickness is greater then misfit dislocations will be formed to accomodate plastically some of the lattice mismatch. Several sources of dislocation have been considered [Matthews et al (1976), Fritz et al (1988), Yamaguchi et al (1989), Nishioka et al (1988)]. The operation of the source is dependant upon its energetic considerations, the more consuming the source the least likely it will be to operate. The first source to operate will be dislocations threading up from the substrate through the epilayer to the surface. They are forced to bow at the strained interface with the threading end gliding laterally to create a segment of misfit dislocation. The mechanism operates for as long as the force acting on the dislocation due to the strain field exceeds the line tension of the defect. The basis for this calculation has been outlined by Matthews et al (1976). When this source of dislocations has been exhausted it may still be

© 1989 IOP Publishing Ltd

neccessary to generate further misfit dislocations. This may take place in a continuous fashion by the multiplication of existing misfit segments or in a discrete manner by the activation of a new source, most likely heterogenous surface loop nucleation. If this were the case then a second critical thickness, the layer thickness above which this dislocation nucleation takes place, would need to be achieved. Energy balance arguments can be used to give values for this type of mechanism [People and Bean (1985)]. The distinction between the effects outlined above is of practical importance since a lattice mismatched layer that is grown onto a buffer layer containing many threading dislocations can act as a defect filter if it is thick enough to turn over threading dislocations incident upon it but not thick enough to generate additional defects. These dislocation filters only have a finite capacity for turning over dislocations since as more dislocations form segments in the interface the strain in the layer is reduced, rendering the mechanism less effective. It is by consideration of the critical thickness effects that we have designed a variety of samples where defect introduction and subsequent removal enables optimum strain relief with minimum defect density in active device areas. This excercise could only be achieved by the use of TEM to monitor the condition of plastic deformation.

2. EXPERIMENTAL

All samples were grown by MOVPE at either low or atmospheric pressure. The general device structure is shown in Figure 1. A variety of buffer layer configurations were used the profiles of which may be seen in Figure 2. The change in lattice parameter in this figure was directly a result of changing the In fraction of the $Ga_xIn_{1-x}As$. The samples were examined by plan view and cross-section TEM using a JEOL 120 CX operated at 120 kV. Reverse bias leakage current, Ir, was used as a measure of material quality. Quantum efficiencies were measured over the 1.6 to 2.4 micron wavelength range. The practical details of obtaining these are published elsewhere [Moseley et al (1986), Scott et al (1986)].

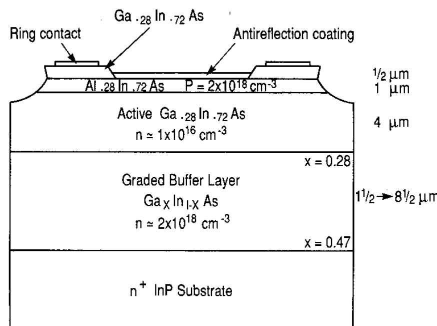

Figure 1: General detector structure used.

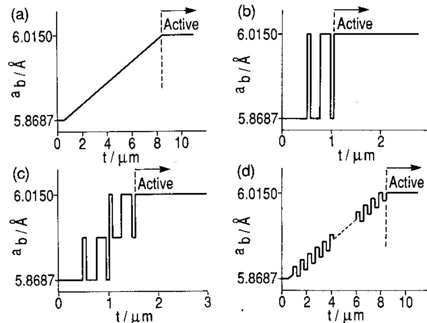

Figure 2: Buffer layer configurations. Lattice parameter, a_b, vs thickness,t.

3. CONSIDERATION OF CRITICAL THICKNESS EFFECTS

The calculation of the critical thickness effects for a graded layer are similar to the calculations for a single strained layer except that expressions for the areal strain energy and the force exerted on the threading dislocation are altered. The buffer layers shown in Figure 2 are designed as intermediate layers, between the substrate and active area, where all changes in lattice parameter are accomodated by plastic deformation. In all cases the existing substrate

threading dislocations will be the first operative misfit dislocation source. Ideally, the residual threading defect density should be better than 10^6 cm^{-2}. For our detector with linear graded buffer {a} this intermediate layer has the disadvantage that there is no control over where the dislocations are generated or turned over. Some dislocation reduction will take place by a mechanism of natural wastage, that is annihilation when dislocations of opposite Burgers vector meet. Kroemer et al (1989) have shown that the dislocation density has a reciprocal relationship with the distance from the point of nucleation. For a linearly graded region in which dislocation nucleation occurs throughout the layer the density is unlikely to be reduced to the required value. If a modulated grade {d} is used such that as well as the long range grade short range changes in composition are incorporated, sufficient to exceed the energetic barriers to lateral glide and hence misfit dislocation generation from existing threading dislocations, then although further dislocation nucleation may take place as a consequence of the grade these may be forced to turn over as soon as they are nucleated. A similar though more severe approach is shown in intermediate layers containing variable mark space Strained Layer Superlattices (SLS) {b and c}. One other method is by the elimination of the graded step altogether and to grow the $Ga_{.28}In_{.72}As$ layer directly onto the InP substrate using an intermediate layer of many SLS to filter the dislocations. This approach is analogous to that used for growing GaAs on Si [Bradley et al (1988)] and will be reported elsewhere.

4. TEM CHARACTERISATION

Removal of the two capping layers by etching enabled plan view TEM analysis of the active device region. Figure 3 shows bright field micrographs corresponding to the four buffer layer configurations outlined above. Figure 2a corresponds to 3a, 2b to 3b and so on. Clearly apparent is the decrease in defect density from a to d. The micrographs correspond to densities

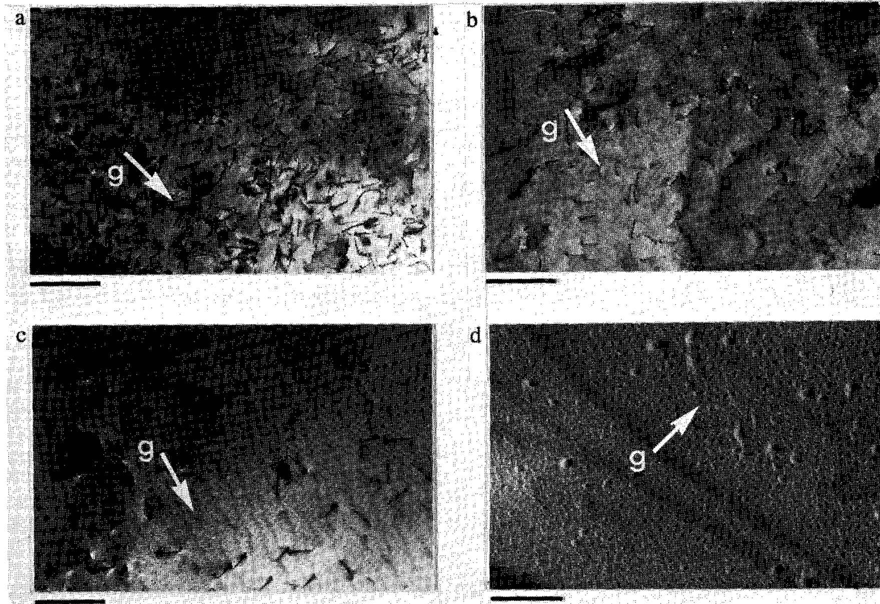

Figure 3: Corresponding (001) plan view dislocation densities of the structures shown in Figure 2. The scale marker = 1 micron and g=<220>.

of $2.7x10^9$, $1.1x10^9$, $2.0x10^8$ and $3x10^6$ dislocations cm^{-2}. The defects, in all the samples, are predominently 1/2<110> threading dislocations with the Burgers vectors at approximately 60^0 to the defect line. Sharply inclined near edge dislocations, again of 1/2<110> type, and stacking faults, formed by the dissociation of threading defects, are also present in lower densities. The difference in defect density is a direct result of the efficiency of the buffer layer in containing the dislocations. The modulated buffer system clearly exhibits the lowest defect density and the linearly graded sample the highest. We have predicted above that the modulated system should contain the lowest density for two reasons. Firstly, substrate dislocations will be turned, almost immediately, into the interface of the thin layers comprising the modulated grade. The individual layers were nominally 100Å thick and contained elastic strain, ß, where ß~0.4%. Secondly, and more importantly, any defects generated will be immediately turned into the interface where they have a chance to react and annihilate. Augustus et al (1988) have shown that SLS filters, used in the GaAs on Si system, are relatively inefficient for removal of defects when densities are low. An approximate guide to efficiency is that both a 1 micron layer containing 4 defect networks and a 4 micron layer with no defect filters contain the same density, 10^8 cm^{-2}, of threading defects. To overcome this inefficiency we must provide many interfaces for the defects to be forced into. It is clear from Figure 4 that we have achieved this for the modulated grade sample. Despite extensive investigation it is not apparent where defects have been generated. However, our observations identify many networks of dislocations lying in misfit relieving orientations approximately every 0.2 micron throughout the buffer. The small separation of these networks will also contribute to the stability of the system via network to network strain relief. The specimen examined in figure 4 was tilted toward the [111] pole to bring the interfaces into view. The dislocations labelled (a) in the figure are within the plane of the interface, (001). They run in orthogonal [110] and [$\bar{1}$10] directions and are of 60° type. The dislocation labelled (b) is inclined and threading through the epilayers. Its path is not deviated, in the field of view, by the shear stress generated at any of the interfaces between the thin layers comprising the grade, unlike the dislocation labelled (c). All the defects examined in cross section had inclined Burgers vectors where b=1/2[101], 1/2[10$\bar{1}$], 1/2[011] or 1/2[01$\bar{1}$]. Clearly operating is a mechanism by which the defects are being deviated from their path and forced into networks which have a misfit relieving orientation. The threading defects that are not deviated comprise the active area defect density measured by plan view. Figure 5 shows in cross section part of the buffer layer of the linearly graded sample. Again the specimen has been tilted toward the [111] pole. Approximately every 0.5 micron a planar array of defects was detected, these denoted by (a) in figure 5. These consisted of both mixed and edge type dislocations and often loops with (001) habit were observed. After 3 micron of growth, at the point b shown in Figure 5, plastic deformation occured at a vastly accelerated rate. No compositional changes could be detected by dark field g_{400} imaging. It is unclear as to the

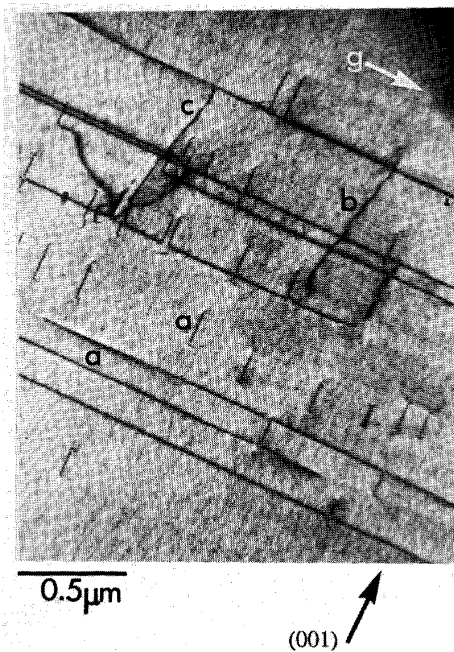

Figure 4: Cross section of the modulated grade sample. Note the (001) direction; g=[$\bar{2}$20].

exact mechanisms of deformation, however, we may conclude from these observations that a series of relaxations have occurred throughout the graded layer, the position of each governed by the stress content of the layer and the energetics of the deformation mechanism. The location of these dislocations could be determined by a stepwise characteristic of what is nominally a linear grade. After a certain thickness an energetic barrier to further elastic deformation has been exceeded incurring massive plastic deformation of the crystal. This may result from an attempt to 'correct' for residual elastic stress present in the preceeding layers. This behaviour was noted for samples grown by both low and atmospheric pressure MOVPE.

Figure 5: Cross section of the linear graded sample. The extent of plastic deformation accelerates after b; g=[$\bar{2}$20]

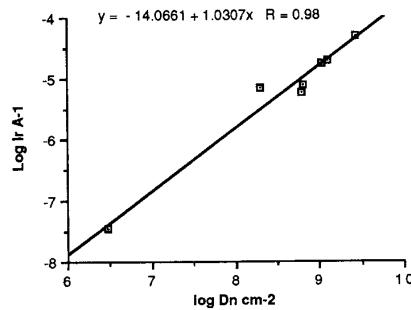

Figure 6: Dislocation density, Dn, vs reverse bias leakage current, Ir.

5. ELECTRICAL CHARACTERISATION

The reverse bias leakage current, Ir, was measured at -0.5V for all the samples fabricated. The threading dislocation density, Dn, was measured by plan view TEM. Figure 6 shows a plot of log(Ir) vs log(Dn). Linear regression of the log-log plot revealed a greater than 98% explained variance by the calculated line, indicative of a very close relationship between the two parameters. Hence, over this range of dislocation densities, threading dislocation density may be used as a predictor for Ir. Similar evidence has been published for GaAsP LED samples [Darby (1979)]. In contrast, however, only weak dependance has been reported for the dc electrical characteristics of HBT structures [Fitzgerald (1988)] where planar defect densities have been measured by cathodoluminescence and TEM.

The sample with the modulated buffer grade exhibited the best dark current, 35nA at -0.5V. Typical capacitance values of 4pF were obtained with a foward resistance of less than 3Ω. Broadband spectral response with peak efficiencies as high as 95% over the 1.7 to 2.25 micron wavelength were recorded. The long wavelength cutoff occured at 2.4 microns. These results contrast sharply with the linearly graded samples where quantum efficiencies were between

30% and 50% and leakage currents typically several tens of microamps. The samples containing the variable mark space SLS displayed only marginally better electrical characteristics than the linearly graded samples. The performance of the detector with the modulated grade, to the best of our knowledge, still represents the highest value of quantum efficiency, and the lowest dark current, reported for detectors operating in this wavelength range.

6. CONCLUSIONS

High quantum efficiency, low leakage current, lattice mismatched GaInAs/AlInAs heterojunction photodiodes have been fabricated by the use of novel graded buffer structures. Threading dislocation generation is inevitable when fabricating materials with this lattice mismatch. The containment of these dislocations was shown to be the key method by which the material quality could be improved to yield device efficiencies in excess of 95% out to 2.2 microns coupled with low dark currents. A clear correlation between the dark current and the threading dislocation density in the active region has been established. The methods of defect generation and filtration were assesed by TEM. Deformation mechanisms for the structures were unclear, but the extent of plastic deformation could be determined by the buffer system chosen. The TEM results clearly explain the observed electrical characteristics of device performance. These results demonstrate clearly the potential of mismatched heterostructure using dislocation engineering for optical detectors for wavelengths in excess of 3 microns.

ACKNOWLEDGEMENTS

The authors wish to thank P D Hodson and R H Wallis for their innovation. J R Riffat, J I Davies, M D Scott and A H Moore for aspects of materials growth. One of the authors, (PK), acknowledges Professor P J Goodhew for stimulating discussion. This work has been carried out with the support of the Procurement Executive, Ministry of Defence, approved by RSRE.

REFERENCES

Augustus P D, Kightley P, Bradley R R and Griffiths R J M Proc. NATO workshop for advanced semiconducting materials. Bristol (1988).

Bisaro R, Merenda P and Pearsall T P 1979 Appl.Phys.Lett. 34 100

Bradley R R, Joyce T B, Beswick J A, Kightley P and Griffiths R J M 1988 Proc. IEE colloq.on GaAs on Si.

Darby D B PhD Thesis 1979 Oxford University.

Dodson B W 1988 Appl.Phys.Lett. 53 394

Fitzgerald E A, Ast D G, Kirchner P D, Pettit G D and Woodall J M 1988 J.Appl.Phys. 63 693

Fritz I J , Gourley P L, Dawson L R and Schriber J E 1988 Appl. Phys.Lett. 53 1098

Kroemer H, Liu T-Y and Petroff P M 1989 J.Cryst.Growth 95 96

van der Leur R H M, Schelleringerhout A J G, Tuinstera F and Mooij J F 1988 J.Appl.Phys. 64 3043

Matthews J W 1975 J.Vac.Sci.Technol. 12 126

Matthews J W, Blakeslee A E and Mader S 1976 Thin Solid Films 33 253

van der Merwe J H 1963 J.Appl.Phys. 34 123

Moseley A J, Scott M D, Moore A H and Wallis R H Electron.Lett .22 1206

Nishioka T, Itoh Y, Sugo M, Yamamoto A, Yamaguchi M 1988 Jap.J.Appl.Phys. 27 L2271

People R and Bean J C 1985 Appl.Phys.Lett 47 322. See also People R and Bean J C 1986 Appl.Phys.Lett. 49 229 Erratum.

Scott M D, Moore A H, Moseley A J and Wallis R H 1986 J.Cryst.Growth. 77 606

Yamaguchi M, Nishioka T and Sugo M 1989 Appl.Phys.Lett. 54 24